DOI: 10.5604/01.3001.0010.4574

STUDY OF DEGRADATION AND GRANULAR FLOW PROCESSES USING X-RAY IMAGING

Laurent Babout[1], Krzysztof Grudzień[1], Marcin Janaszewski[1,*], Łukasz Jopek[1,*]
[1]Institute of Applied Computer Science, Lodz University of Technology, *Formerly at the Institute of Applied Computer Science

Abstract. *This paper reviews the work that has been done in the past 10 years at the Lodz University of technology about the visualization and the quantification of phenomena related to degradation processes (i.e. stress corrosion cracking in stainless steel, fatigue crack in titanium alloys) in engineering materials as well as granular flow in silos using X-ray imaging (i.e. radiography and (micro)tomography). Besides presenting the experimental protocols, the paper also presents the image processing strategies that have been applied to enable the extraction of characteristic parameters from the volumetric images.*

Keywords: X-ray imaging, damage, gravitational flow, image processing.

ANALIZA PROCESÓW DEGRADACJI I PRZEPŁYWU GRANULATU Z WYKORZYSTANIEM OBRAZOWANIA METODĄ PROMIENI X

Streszczenie. *Artykuł przedstawia przegląd prac badawczych przeprowadzonych w ostatnich 10 latach w Politechnice Łódzkiej, dotyczących wizualizacji oraz analizy ilościowej zjawisk mających miejsce w procesie degradacji materiałów (tj. korozji naprężeniowej stali nierdzewnej, pęknięcia stopów tytanu) oraz przepływu materiałów sypkich w silosach z wykorzystaniem obrazowania metodami opartymi na promieniowaniu X (tzn. radiografii oraz (micro)tomografii). Oprócz przedstawienia metodologii pomiaru, zostały również opisane metody przetwarzania obrazów, pozwalające na wyznaczenie charakterystycznych parametrów badanych procesów z obrazów wolumetrycznych.*

Słowa kluczowe: obrazowanie metodą promieni X, przepływ grawitacyjny, przetwarzanie obrazów

Introduction

Other the past 15 years, X-ray tomography has become a mature non-destructive technique to study internal structure of materials in various fields of applied science (e.g. biomedical engineering, geology, civil engineering or materials science engineering). This has been supported by the constant effort of researchers to push forward both the spatial and temporal resolutions of the technology to the highest. One can chronologically cite the works on increased contrast using phase shift [11, 25], nanotomography [30], (ultra)fast X-ray (micro)tomography [9, 13, 23, 28] or diffraction tomography/microscopy [19, 21, 27, 29]. Besides, the possibility of carrying out diverse types of in situ test (mechanical, environmental) has given the scientists the unique chance to closely investigate the changes over time of the bulk of the objects of interest. However, one of the main drawbacks of X-ray tomography, especially during time lapse or continuous studies is the tremendous amount of data generated that need to be interpreted (a typical tomography scan represents around 8 Gb of memory). Therefore, automated processing of the data is needed to facilitate their characterization.

This paper presents the work that has been carried out by the authors in the past 10 years dealing with time lapse study of degradation processes in engineering material as well as flow processes in granular materials. A focus is also done on the image processing steps that have been thought in order to carry out quantitative characterization of the phenomena undergone by the materials of interest. After briefly presenting the technology at synchrotron and laboratory level, the paper presents 3 different studies in Section 0 dealing with intergranular stress corrosion cracking in austenitic stainless steel, short fatigue crack propagation in lamellar titanium alloy and, finally, silo discharging of cohesionless dry sand. Main image processing and analysis methods are also introduced to the readers, highlighting their importance to extract complex features from the 3D images.

1. Experimental set-ups

The general concept of X-ray tomography is an extension of classical X-ray radiography, and is based on the attenuation of the X-ray beam through the specimen. By acquiring a set of radiographs at different rotation steps of the specimen over 180° or 360°, one can reconstruct the volume of the object using well-known filtered back-projection algorithm [20]. To do so, an X-ray tomography set-up will need three basic equipment elements: an X-ray source (synchrotron light source or electron gun, as mentioned later), a rotation stage where the sample is mounted and a detector, usually combining a fluorescent screen, which converts X-rays to visible light and a set of optic lenses that transfers the light to a CCD camera. Usually, the X-ray beam can be parallel or divergent with a cone shape.

1.1. X-ray microtomography at the European Synchrotron Radiation Facility

Synchrotron radiation facilities are common large-scale scientific infrastructures (APS in the USA, SPRING8 in Japan, DIAMOND in the UK, SOLEIL or the ESRF in France) where X-rays are used to study the matter from different perspectives. For instance, using X-rays at different wavelengths, one can investigate the crystallographic composition of the matter (e.g. using diffraction, spectroscopy, SAXS), its electronic structure and magnetic properties (inelastic scattering, absorption spectroscopy) or its internal structure using X-ray micro/nanotomography.

X-ray synchrotron tomography equipment is usually characterized by a high energy, coherent X-ray beam, which can be monochromatic or polychromatic, depending of the application. For instance, a monochromatic beam will enable to avoid artifacts problems such as beam hardening, hence resulting in images of very high quality, but at limited temporal resolution (typically 1 scan / 15 minutes). However, polychromatic beam will be preferable if continuous scanning is needed (e.g. 1 scan / s), for instance to investigate microstructural changes with temperature, since the X-ray flux will be tremendously larger than for monochromatic beam. The fact that the beam is coherent also gives the possibility to go around the problem of low absorption contrast encountered in some cases such as Al/SiC composites, by enabling to create on the detector so-called phase contrast [11]. Note that the two first studies presented in this paper have been carried out at the X-ray microtomography beamline ID19 of the ESRF (Fig. 1).

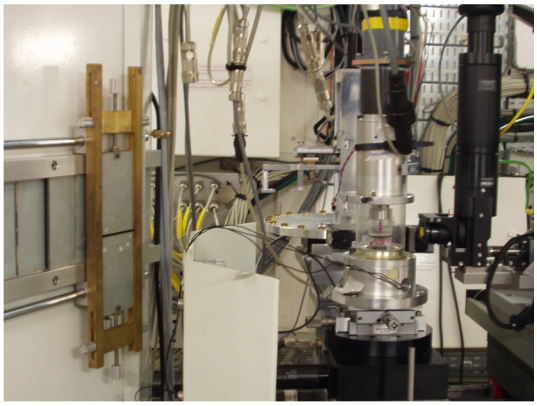

Fig. 1. View of the X-ray microtomography hutch at ID19 (ESRF)

1.2. X-ray tomography laboratory kits

Since the technique has become very popular and the access to synchrotron sources more and more difficult (proposal success rate lower ~10%), numerous companies have developed X-ray tomography laboratory kits dedicated to universities and the industry, mainly for non-destructive inspection for the latter. Classical units, but also more advanced ones (e.g. custom bay for large engineering component investigation or X-ray nanotomography) have been developed to meet customers' need. All are using electron guns as the source to generate X-rays when the electrons, which are collimated using magnets, hit a metal target. Cone X-ray beam are mainly generated in such type of tomography devices. As an example, one can cite the Henry Moseley X-ray Imaging Facility (HMXIF) at the University of Manchester, which owns more the five different X-ray tomography lab kits produced by Zeiss Xradia or Nikon metrologies, in order to investigate objects of different size (up to 30 cm diameter) at different spatial scales (from 100 nm to 100 µm spatial resolution). One of these tomographs is shown in Fig. 2. Note that the third study presented in this paper has been partly performed at this X-ray imaging center.

Fig. 2. View of a Nikon X-ray tomography device owned by the University of Manchester

2. Example of case studies

2.1. Intergranular stress corrosion cracking in stainless steel

The objective of this research study was to investigate how a crack induced by the dual effect of corrosion and external loading (stress corrosion cracking) develop in austenitic stainless steel. The literature predicts that the crack will develop in an intergranular manner for polycrystalline materials such as stainless steel, however nothing was really mentioned about the presence of bridge ligament along the crack path that can be correlated with special low angle grain boundaries.

In that context, Intergranular stress corrosion cracking in a sensitized type 302 stainless steel wire has been observed in situ using high resolution X-ray microtomography. The details of the experimental set-up, which is depicted in Fig. 3, is presented in details in [6]. The spatial resolution was 0.7 µm.

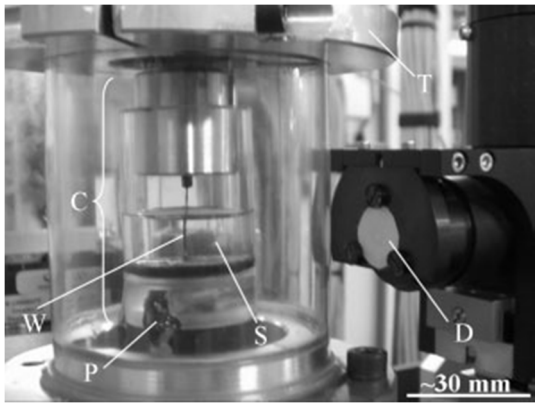

Fig. 3. X-ray microtomography set-up on ID19 for in situ IGSCC experiment presented in [6]. *W: 302SS sample wire, P: platinum counter electrode, S: acid solution, T: tensile machine, D: X-ray detector*

Fig. 4 shows typical images of the crack development during IGSCC. Firstly, one can notice that the cracks have developed from the outside of the sample to the inside (Fig. 4a). Secondly, the crack pattern is intergranular and reveals the presence of grains revealing the polycrystalline nature of the austenitic stainless steel microstructure (Fig. 4a). Thirdly, the crack presents discontinuities along its path, as marked by white circles in Fig. 4a-b, which correspond in 3D to so-called bridge ligaments. The main goal of the study was to detect and extract such feature from the 3D images using dedicated image processing method described below.

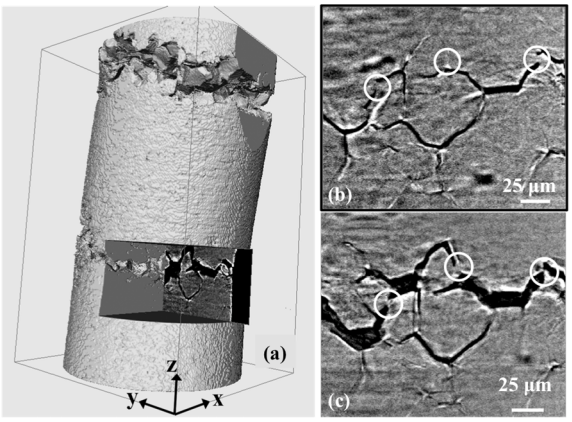

Fig. 4. (a) 3D view and (b-c) sequence of cross-sections showing the development of IGSCC in stainless steel at two different loading time. White circles highlights the presence of bridge ligaments along the crack path. Rearranged from [6]

As it can be seen in Fig. 4a, the crack has developed from the surface of the sample. It is easy to understand that the crack is not a subset of the space since connected to the background. In order to segment it, we have applied the minimal surface for maximal flow algorithm developed by Appleton and Talbot [2] and modified by Kornev et al. [22]. Based on the weighted graph theory, the method simulates the flow of an ideal fluid with isotropic velocity constraints by iteratively updating conditions related to pressure at vertices and inward/outward flow at edges of the graph, the latter being constrained by a function inversely proportional to the gradient of the image. By using a binary source located inside the object to be segmented and a sink which surrounds it, the object volume grows until a energy function, which integrate the normal of the local flow at each point of the object surface is minimized. This is illustrated in Fig. 5, where one can see that the crack is not separated from the background.

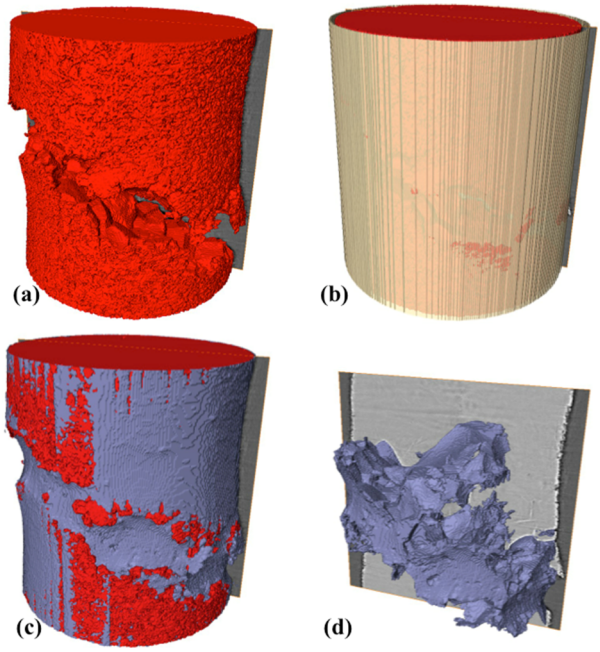

Fig. 5. Application of the minimal surface for maximal flow algorithm to segment open crack. (a) sample serving as source, (b) the sink, (d) the minimal surface and (d) the extracted crack

The reliable extraction of bridge ligaments from X-ray microtomography data requires an image processing strategy. Standard methods, such as histogram-based segmentation, will not isolate the bridges from the material. Indeed, after segmentation of the crack, bridges correspond to holes (or tunnels) in the crack and are part of the surrounding background. Since algorithms to close holes in 3D objects exist, these may be used to extract bridges.

The problem of hole closing is considered in the literature within the general topic of repairing 3D models. Several methods have been developed to correct defects in isosurface and 3D meshes, as mentioned in [17, 18]. One approach, called the Hole Closing Algorithm (HCA), is particularly well suited to detecting holes in a 3D object, such as a bridge ligaments across a crack [1]. The method is based on topological considerations, such as topological number, topology preservation and simple points that are common concepts used in thinning algorithms [12, 26]. The methods has been extended to take into account the thickness of the object surrounding the hole [17] or to close extremities of tunnels [18]. However, the original approach proposed by Aktouf et al. [1] was found to be the most appropriate in the case of bridge ligament segmentation, since by essence holes correspond to portions of grain boundary, which have no thickness, hence represented at most by 3D objects of thickness 1.

Fig. 6 shows an example of the application of the HCA to extract bridge ligaments from a portion of an IGSCC and published in [5]. Investigation of the geometric orientation of the ligaments have shown that many bridges are located on grain boundary facets with the angle between their normal and the loading direction larger than 60°. Note that a study that compared this tomography data with crystallographic orientation of the grains obtained by DCT did not clearly verified the correlation between bridge ligament formation and low Σ boundaries [24], which confirm the complex nature of this degradation process and the challenges that still need to be tackled to understand it.

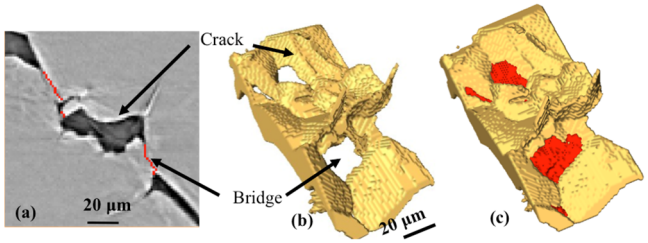

Fig. 6. Hole closing algorithm (HCA) in action. (a) 2d cross section showing crack and bridge. (b) 3D view of the crack showing holes. (c) Holes corresponding to bridges closed using HCA. Rearranged from [5]

2.2. Short fatigue crack in fully lamellar Titanium alloy

The second example of this paper concerns work that has been carried out on short fatigue crack propagation in (α+β) Titanium alloy with fully lamellar microstructure. The main objective was to investigate the interaction of the crack path with the microstructural features of this engineering material, which are the β grain boundaries and the α colonies. Once again, 3D *in situ* investigation was chosen to obtain a non ambiguous set of information, as the crack, initiated at the surface of the sample, propagates in the bulk of the material and strongly interacts with the microstructure.

To do so, an especially designed fatigue machine, depicted in Fig. 7a, was mounted on ID19. Details of the experiments are presented in [10]. The spatial resolution was 0.7 µm as in the previous study (Section 2.1). An exemplar 3D image of the crack branches interacted with the microstructure is shown in Fig. 7b. One can particularly distinguish the deflection of the crack (crack 1) when it has crossed a boundary between 2 α colonies (indicated by dashed curves).

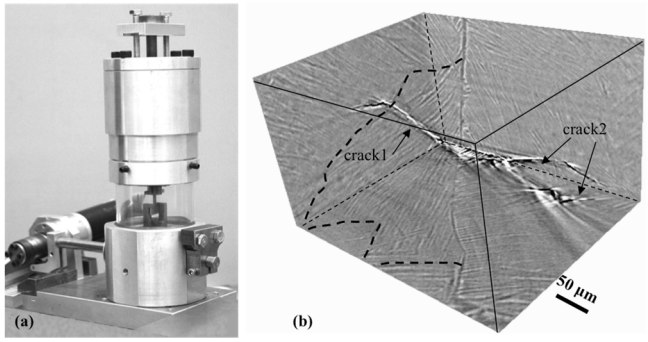

Fig. 7. (a) view of the in situ fatigue machine used for experiment (Courtesy of J.-Y. Buffiere (INSA-Lyon, France)). (b) Visualization of the crack interaction with the Ti lamellar microstructure after 27k fatigue cycles [8]

Because the lamellar microstructure is very complex and can be very tedious to analyze, an image processing strategy has been thought to segment both the crack and the microstructural features mentioned above. Since the lamellar microstructure can be seen as a directional textured image, a directional filter bank with special structuring element presented in Fig. 8 has been thought to capture the local directionality of the lamellae that have nearly planar shapes [3]. The 3D image is convolved with the 13 independent directional filters shown in Fig. 8c and the argument of the maximum response (i.e. the index of the main direction) is selected for each voxel of the image.

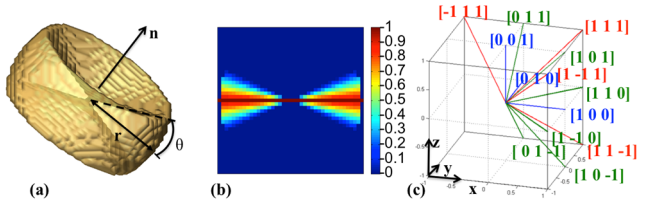

Fig. 8. (a) Isosurface of the CHG filter. (b) 2D filter kernel profile. (c) Bank of principal filter normal directions [3]

The directional filter bank has also shown its utility in the segmentation phase of β-grain boundary (β-gb) [4] and partitioning of the fatigue crack. This is based on the fact that all 3 features correspond to surface objects (their skeleton is a two-dimensional, topological manifold) and present different orientations.

Having segmented the 3 features separately, the last step consists in merging them in the same volume using image registration based on pose estimation (Fig. 9a), since the creation of the crack hinders the segmentation of the Ti microstructure in the tomography scan after fatigue cycling. The quantitative analysis of the interaction between the crack and the TI microstructure can now be performed, as it was described in details in [8]. For example, one can see on Fig. 9b that the crack preferentially propagates in colonies in a trans-lamellar way but perpendicular to the lamellar orientation (blue color), even if a significant portion of the crack also propagates in an inter-lamellar way (red portion). This is the first 3D confirmation of this type of propagation and it is highly probable that translamellar crack with very high angle has crossed lamellae favorably oriented for ⟨a⟩ basal slip while interlamellar crack along lamellae favorably oriented for ⟨a⟩ prismatic slip. A next type of study should combine X-ray microtomography of this kind with high-energy diffraction microscopy, a very recent technique that has shown its potential to get local crystallographic orientation of grains in polycrystalline/polyphase materials such as Ti alloy [29].

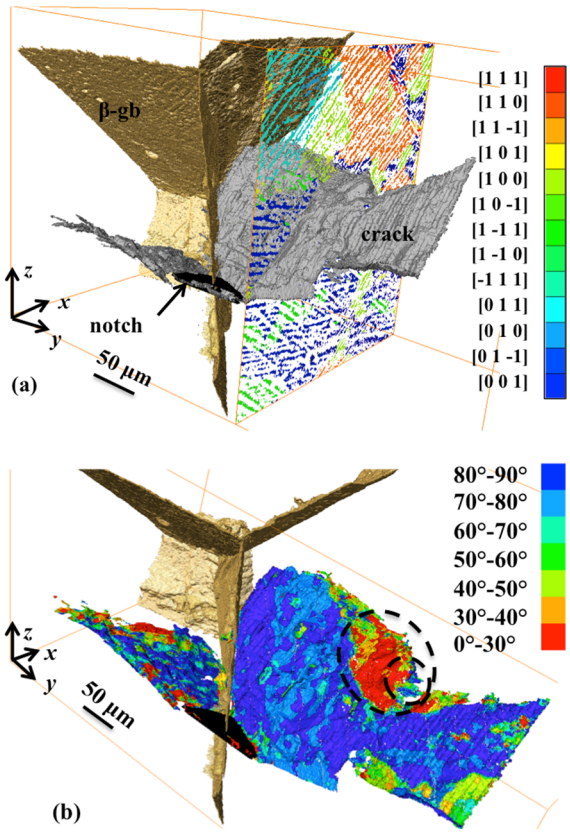

Fig. 9 (a) 3D rendering showing the interaction of the crack with the β grain boundary and the α-lamellae classified w.r.t. their orientation. (b) 3D rendering of the angle between the local crack orientation and lamellar orientation [8]

2.3. Silo discharging of granular materials

The last example presents recent works to investigate dynamic phenomena during silo discharging using X-ray imaging (i.e. X-ray radiography and tomography). This has completed previous Electrical Capacitance Tomography studies performed at the Institute of Applied Computer Science [15, 16]. In all cases were investigated the effect of packing density and silo wall roughness in model rectangular silo.

The first part of the study has concerned silo discharging during mass flow of cohesionless dry sand, looking preferentially to the formation of shear zone at the silo wall during emptying process. This study has been done at the MATEIS laboratory (INSA-Lyon, France) using a GE Phoenix v|tome|x system shown in Fig. 10.

Fig. 10. General view of the X-ray tomography equipment at INSA-Lyon with, in front, the rectangular silo model used for the mass flow study [14]

One of the most important results of the study [14] has shown the pronounced formation of shear zone along silo wall with rough structure depicted in Fig. 11b by red dashed rectangle, as compared with the case of smooth wall. Moreover, the size of shear zone in the case of loose sand packing density seems to be larger than for dense sand. This difference is a direct effect of the increase of sand concentration for loose sand in the whole silo bin section except in the area at the silo wall. In the case of initially dense packing, the concentration in the whole bin section decreases and the difference between the shear zone and the rest of the silo is not as large as for the initially loose sand packing. Another noticeable and obvious dissimilarity between the two packing is the time required to empty the silo. In the case of dense sand, the discharging duration is larger than for loose sand (i.e. typically more about 5 s), as the initial amount of sand for the same height of packing is larger.

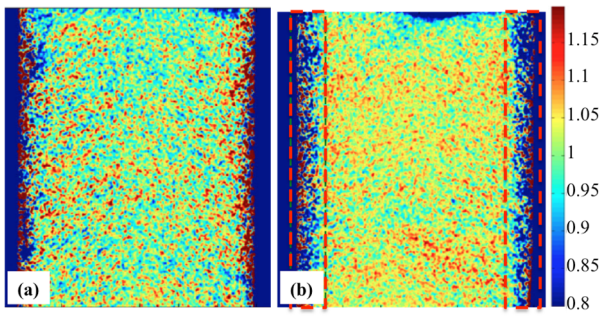

Fig. 11. 2D normalized X-ray radiographs of sand concentration distribution after 1 s of the silo discharging process, (a) loose sand and smooth silo wall, b) loose sand and rough silo wall [14]

A more recent study has focused on the second type of concentric flow, namely funnel flow [7] and was carried out at the HMXIF center at the University of Manchester and experiments were done using a Nikon X-Tek custom 320kV bay. Again, main-

ly X-ray radiography data have been studied to identify the phenomena of funnel creation and geometric characteristics that can be related to the initial packing density of dry sand. Still, time lapse X-ray tomography was also performed to show the evidence that funnel formation, as well as particle tracking during the emptying process could be analyzed.

As far as the initially dense packing is concerned, one can see in Fig. 12 the remarkable contrast between the flow zone and the stagnant ones, greatly facilitating their quantitative study, as explained in [7]. However, the X-ray tomography data have revealed that the width of the funnel flow is not linear along the depth of the silo, but has a rather convex shape, that is to say with a width smaller at the front and back walls of the silo than in the middle. Moreover, studies of different definition of funnel widths, as proposed in Fig. 13, have shown that the most accurate calculation is done when the width is considered at half of the distance from the outlet to the dip (or V-shape) of the upper surface.

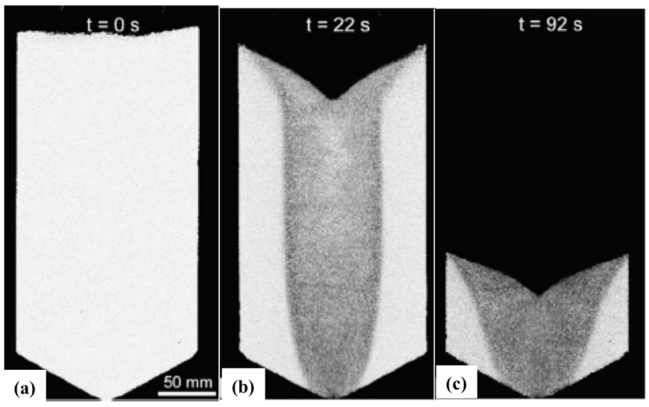

Fig. 12. Sequence of rescaled radiographs highlighting funnel flow for initial dense packing of quartz sand [7]

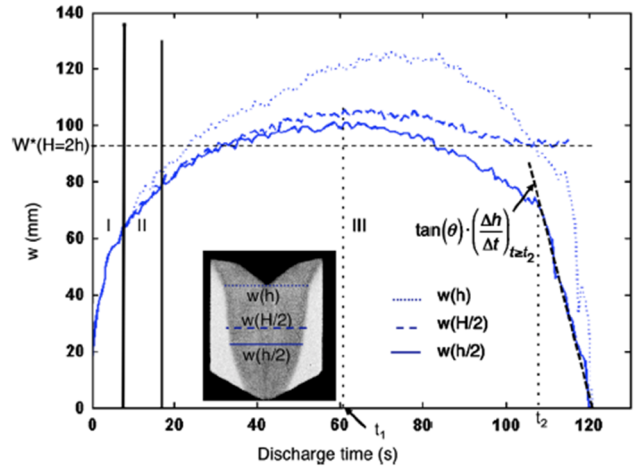

Fig. 13. Evolution of silo width parameters vs. discharge time for the case of dense packing with smooth walls as illustrated in the embedded radiograph. The width W corresponds to the special case when the height at the dip h is 2 times less than the full height H. The trend line, together with the corresponding slope equation of the last part of the width profile w(h/2) when it reaches the hopper wall (i.e. $t=t_2$), is also shown* [7]

As far as the initial loose sand packing is concerned, the flow characteristic is different with so-called semi-mass flow process, that is to say a combination of mass flow at the top of the bin and presence of stagnant zone in the bottom, as pictured in the sequence presented in Fig. 14. One should bear in mind that good visualization of the stagnant zone was only possible by substracting consecutive radiographs (to reveal flow zone w.r.t. stagnant zone) and processing local variance calculation in the image to better reveal the presence of granular concentration fluctuation in the flow zone. Studies of the height of the stagnant zone was therefore made possible and revealed interesting aspects of the semi-mass flow, as shown in Fig. 15. Firstly, the initial height of the stagnant zone H_{SZ} (that is just after the outlet has been opened) is larger for rough wall than for smooth wall conditions, and can be attributed to the increase of particle-wall friction when the wall gets rougher [31]. Secondly, H_{SZ} increases as the discharging time increases (and the height of the bin H_b decreases), until the height of falling material $(H_b(t^*)–H_{SZ}(t^*))$ is about 20% of the initial material height H_b. However, the increase rate is smaller for rough wall and was attributed to the formation of a shear zone with larger wall friction due to the presence of the sand papered wall, which induces movement of the material away from the wall, reducing the possibility of accumulation of sand at the top of the stagnant zone. After t^*, the flow is rather similar to a funnel flow and the decrease of the height H_{SZ} is not dependent on the roughness of the wall. Again, all these valuable quantitative analysis was made possible thanks to appropriate post processing of the radiography images to increase the contrast between stagnant and flow zones.

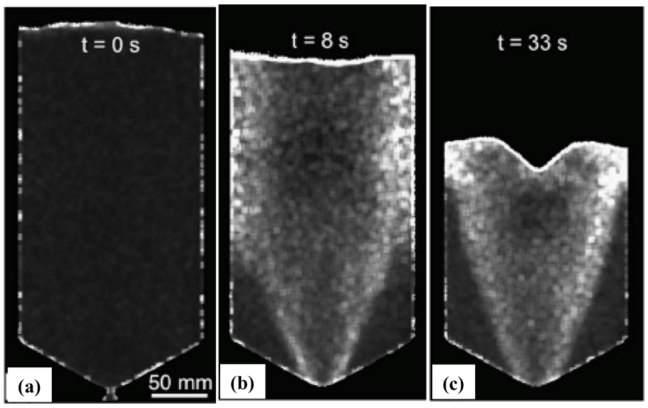

Fig. 14 Sequence of rescaled radiographs highlighting semi-mass flow for initial loose packing of quartz sand [7]

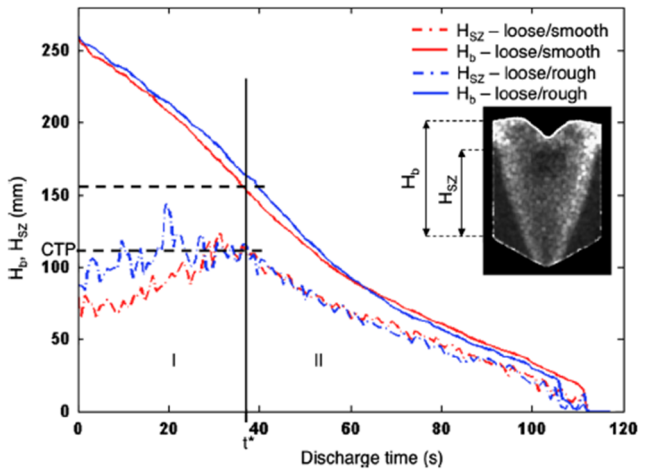

Fig. 15. Change in stagnant zone and funnel dimensions vs. discharge time during complete silo emptying for loose packing within the silo with smooth and rough walls [7]

3. Conclusion

This paper has presented three case studies of physical processes using X-ray (micro)tomography that are, we believe, emblematic of the research interests of the Institute of Applied Computer Science. These will not have been possible without strong collaboration with researchers from INSA-Lyon and the University of Manchester, the two European universities leading the work of materials characterization using X-ray imaging. An important message of the paper is also that, without properly chosen image processing and analysis methods, it is barely impossible to retrieve non-ambiguous quantitative characterization from the material of interest.

Acknowledgments

The authors would like to mention the different grants, which partly financed the work presented in this paper: FP6 Marie Curie DENIDIA project (MTKD-CT-2006-039546) and Polish grants from the Ministry of Science and Higher Education (3687/B/T02/2009/37 and 6522/B/T02/2011/40).

References

[1] Aktouf Z., Bertrand G., Perroton L.: A three-dimensional holes closing algorithm. Pattern Recognition Letters, 23/2002, 523–531.
[2] Appleton B., Talbot H.: Globally minimal surfaces by continuous maximal flows. IEEE Transactions on Pattern Analysis and Machine Intelligence, 28/2006, 106–118.
[3] Babout L., Jopek L., Janaszewski M.: A New Directional Filter Bank for 3D Texture Segmentation: Application to Lamellar Microstructure in Titanium Alloy, in 13th IAPR International Conference on Machine Vision Applications, 2013, 419–422.
[4] Babout L., Jopek L., Janaszewski M.: Extraction of complex microstructural patterns in X-ray microtomography images: application to lamellar titanium alloy, in 7th World Congress on Industrial Process Tomography (WCIPT7), 2013, 703–712.
[5] Babout L., Janaszewski M., Marrow T. J., Withers P. J.: A method for the 3-D quantification of bridging ligaments during crack propagation. Scripta Materialia, 65/2011, 131–134.
[6] Babout L., Marrow T.J., Engelberg D., Withers P.J.: X-ray microtomographic observation of intergranular stress corrosion cracking in sensitised austenitic stainless steel. Materials Science and Technology, 22/2006, 1068–1075.
[7] Babout L., Grudzien K., Maire E., Withers P. J.. Influence of wall roughness and packing density on stagnant zone formation during funnel flow discharge from a silo: An X-ray imaging study. Chemical Engineering Science, 97/2013, 210–224.
[8] Babout L., Jopek Ł., Preuss M.. 3D characterization of trans- and inter-lamellar fatigue crack in (α+β) Ti alloy. Materials Characterization, 98/2014, 130–139.
[9] Bieberle MBarthel., F., Menz H.-J., Mayer H.-G., Hampel U.: Ultrafast three-dimensional x-ray computed tomography. Applied Physics Letters, 98/2011, 034101.
[10] Birosca S., Buffiere J.-Y., Garcia-Pastor F. A., Karadge M., Babout L., Preuss M.: Three-dimensional characterization of fatigue cracks in Ti-6246 using X-ray tomography and electron backscatter diffraction. Acta Materialia, 57/2009, 5834–5847.
[11] Cloetens P., Pateyron-Salome M., Buffiere J. Y., Peix G., Baruchel J., Peyrin F., Schlenker M.: Observation of microstructure and damage in materials by phase sensitive radiography and tomography. Journal of Applied Physics, 81/1997, 5878–5886.
[12] Couprie M., Coeurjolly D., Zrour R.: Discrete bisector function and Euclidean skeleton in 2D and 3D. Image Vision Comput., 25/2007, 1543.
[13] Fischer F., Hoppe D., Schleicher E., Mattausch G., Flaske H., Bartel R., Hampel U.: An ultra fast electron beam x-ray tomography scanner. Measurement Science & Technology, 19/2008.
[14] Grudzien K., Niedostatkiewicz M., Adrien J., Maire E., Babout L.: Analysis of the bulk solid flow during gravitational silo emptying using X-ray and ECT tomography. Powder Technology, 224/2012, 196–208.
[15] Grudzien K., Romanowski A., Chaniecki Z., Niedostatkiewicz M., Sankowski D.: Description of the silo flow and bulk solid pulsation detection using ECT. Flow Measurement and Instrumentation, 21/2010, 198–206.
[16] Grudzien K., Romanowski A., Williams R.A.: Application of a Bayesian approach to the tomographic analysis of hopper fow. Particle and Particle Systems Characterization, 22/2006, 246.
[17] Janaszewski M., Couprie M., Babout L.. Hole filling in 3D volumetric objects. Pattern Recognition, 43/2010, 3548–3559.
[18] Janaszewski M., Postolski M., Babout L.. Robust algorithm for tunnel closing in 3D volumetric objects based on topological characteristics of points. Pattern Recognition Letters, 32/2011, 2231–2238.
[19] Johnson G., King A., Honnicke M.G., Marrow J., Ludwig W.: X-ray diffraction contrast tomography: A novel technique for three-dimensional grain mapping of polycrystals. II. The combined case. Journal of Applied Crystallography, 41/2008, 310–318.
[20] Kak A.C., Slaney M.. Principles of computerized tomographic imaging. New York, 1987.
[21] King A., Johnson G., Engelberg D., Ludwig W., Marrow J.. Observations of intergranular stress corrosion cracking in a grain-mapped polycrystal. Science, 321/2008, 382–385.
[22] Kornev A., Babout L., Janaszewski M., Talbot H.: Outer Surface Reconstruction for 3d Fractured Objects, in Computer Vision and Graphics, Pts 1 and 2, 6374, L. Bolc, R. Tadeusiewicz, L. J. Chmielewski, and K. Wojciechowski, Eds. Berlin: SPRINGER-VERLAG, 2010, 57–64.
[23] Limodin N., Salvo L., Boller E., Suery M., Felberbaum M., Gailliegue S., Madi K.: In situ and real-time 3-D microtomography investigation of dendritic solidification in an Al-10 wt.% Cu alloy. Acta Materialia, 57/2009, 2300–2310.
[24] Ludwig W., King A., Herbig M., Reischig P., Marrow J., Babout L., Lauridsen E.M., Proudhon H., Buffiere J.Y.: Characterization of polycrystalline materials by combined use of synchrotron X-ray imaging and diffraction techniques. JOM, 62/2010, 22–28.
[25] Pfeiffer F., Weitkamp T., Bunk O., David C.: Phase retrieval and differential phase-contrast imaging with low-brilliance X-ray sources. Nature Physics, 2/2006, 258–261.
[26] Saúde A.V., Couprie M., Lotufo R.A.: Discrete 2D and 3D euclidean medial axis in higher resolution. Image and Vision Computing, 27/2009, 354–363.
[27] Spear A.D., Li S.F., Lind J.F., Suter R.M., Ingraffea A.R.: Three-dimensional characterization of microstructurally small fatigue-crack evolution using quantitative fractography combined with post-mortem X-ray tomography and high-energy X-ray diffraction microscopy. Acta Materialia, 76/2014, 413–424.
[28] Suery M., Adrien J., Landron C., Terzi S., Maire E., Salvo L., Blandin J.-J.: Fast in-situ X-ray micro tomography characterisation of microstructural evolution and strain-induced damage in alloys at various temperatures. International Journal of Materials Research, 101/2010, 1080–1088.
[29] Wielewski E., Menasche D.B., Callahan P.G., Suter R.M.: Three-dimensional α colony characterization and prior-β grain reconstruction of a lamellar Ti–6Al–4V specimen using near-field high-energy X-ray diffraction microscopy. Journal of Applied Crystallography, 48/2015, 1165–1171.
[30] Withers P.J.: X-ray nanotomography. Materials Today, 10/2007, 26–34.
[31] Yang Y., Rotter M., Ooi J., Wang Y.: Flow Channel Boundaries in Silos. Chemical Engineering & Technology, 34/2011, 1295–1302.

Prof. Laurent Babout
e-mail: laurent.babout@p.lodz.pl.

Prof. L. Babout obtained his PhD degree in 2002 from INSA-Lyon (France) and DSc degree in 2011 from the Lodz University of Technology (TUL). Currently he holds a position of associate professor at TUL. His scientific interest covers X-ray tomography and 3D image processing, with main focus on materials science applications. Prof. L. Babout is a SIAM member, TMS member and author or co-author of more than 100 scientific papers, books and chapters.

Ph.D. Krzysztof Grudzień
e-mail: kgrudzi@iis.p.lodz.pl

Assistant Professor of Applied Computer Science at Lodz University of Technology. Member of Polish Information Processing Society and ACM Lodz Chapter. He obtained PhD in 2007 in the field of Computer Science, Process Tomography specialty.
His research interests include applications of non-invasive imaging techniques and identification of dynamic industrial processes parameters, development of algorithms for image processing and analysis with particular reference to the analysis of sequences of 2D tomography images gathered from ECT and X-ray tomography systems.

Ph.D. Eng. Marcin Janaszewski
e-mail: marcin.janaszewski.ext@zeiss.com

Contractor in Michael Bailey Associates Group, currently working as Senior Software Developer for Carl Zeiss GmbH, Research and Development Department. He obtained PhD in 2003 in the field of Computer Science. His interests include pattern recognition, image processing, digital topology and geometry, applications of 3D image processing in material science and medicine.

Ph.D. Eng. Łukasz Jopek
e-mail: l.jopek@pixel.com.pl

Software Developer at Pixel Technology (Lodz, Poland). He currently works in a research project, which focuses on segmentation and analysis of medical images. He obtained his PhD in 2014 in the field of Computer Science from the Lodz University of Technology. His interests include pattern recognition, image processing, image texture analysis, applications of 2D/3D image processing in material science and medicine.

otrzymano/received: 20.09.2016 *przyjęto do druku/accepted: 15.02.2017*